Self-diffusion of grains in a two-dimensional vibrofluidized bed

R. D. Wildman,[1,*] J. M. Huntley,[1] and J.-P. Hansen[2]
[1]*Department of Mechanical Engineering, Loughborough University, Loughborough, Leicestershire LE11 3TU, United Kingdom*
[2]*Department of Chemistry, University Chemical Laboratory, Lensfield Road, Cambridge CB2 1EW, United Kingdom*
(Received 20 April 1999; revised manuscript received 7 July 1999)

The analogy of vibrofluidized granular beds with a thermal gas of hard discs has been tested. Analysis of the mean squared displacement behavior of the grains allowed comparison of the measured diffusion with the predicted value at a particular combination of granular temperature and packing fraction. High speed photography, image analysis, and particle tracking software enabled accurate location of the grains. Appropriate analysis of the three mean squared displacement regimes, ballistic, diffusive, and crossover between the two extremes, allowed both the diffusion coefficient and the granular temperature to be measured at the same packing fraction. Broad agreement between Chapman-Enskog theory relating temperature to self-diffusion and observation was observed up to packing fractions of $\eta \sim 0.7$. At higher packing fractions the grains showed evidence of caging and jump diffusion, with the observed diffusion rapidly diverging from that predicted by theory. Measurement of self-diffusion coefficients and subsequent use of kinetic theory was found to be an accurate method to determine the granular temperature for intermediate packing fractions ($\eta = 0.4 - 0.6$), and would be particularly suitable for those situations where the time resolution of the experimental facility is insufficient to resolve the speed of the grain between collisions. [S1063-651X(99)02012-7]

PACS number(s): 45.70.Mg, 51.10.+y, 05.60.−k

I. INTRODUCTION

Investigation into the behavior of granular materials has uncovered a range of interesting phenomena, many of which have been studied extensively [1]. Theoretical understanding of granular flow began in the 1970's, based on analogies with the kinetic theory of gases [2,3]. One barrier to the successful analysis of granular flow is that the material never reaches ''thermal'' equilibrium, rather, it forms a nonequilibrium steady state. Gas kinetic theory is generally concerned with the relaxation towards equilibrium; hence any analysis of granular flows must assume, and then justify, that the system is sufficiently close to equilibrium for such methods to be appropriate. Recently Campbell [4] pointed out the need for experimental techniques capable of measuring microscopic properties such as granular temperature. In response to this, methods based on high-speed photography [5] and diffusive wave spectroscopy [6] have since been developed to provide such data. These methods have helped to justify assumptions of near equilibrium [5,7].

Vibrofluidized beds of granular materials, such as steel or aluminum balls are an idealization of the mechanical excitation of granular materials found in nature and industry. Warr *et al*. examined the velocity distributions in the x and y directions in a two dimensional granular bed and found that, at low packing fractions corresponding to a few layers in the condensed state, the granular temperature is anisotropic [5,8]. These experiments also revealed that the temperature declines with increasing distance from the base. The average granular temperature of the grains was reported to scale with the velocity of the base as a power law with an exponent of about 1.4. This was in contrast to theoretical predictions. Warr *et al.* and Kumaran predicted a exponent of 2 in the case of dissipation during grain-grain collisions, but Kumaran also analyzed dissipation through viscous drag, in which case the predicted exponent is $\frac{4}{3}$, indicating that the observed exponent could be due to a combination of both forms of dissipation [9,10]. Unfortunately this does not explain the value of the exponents observed during numerical simulations [11]. This has led to some debate, with a number of reasons recently put forward [12,13].

Many authors have highlighted the similarity between fluidized granular materials and thermal liquids. In view of these similarities, it seems likely that the extensive literature on thermal liquids includes results which are likely to be applicable to the flow properties of almost-elastic granular materials at high packing fractions. Molecular dynamics (MD) simulations have proved important in the investigation of transport properties of fluids at high densities. Alder and Wainwright [14] found that in two dimensions the velocity autocorrelation function appeared to decay as t^{-1} at long times, in contrast to the expected exponential decay. This led to significant interest in the high density regime and the collective behavior of liquids [15]. MD simulations have also been used to predict the deviation of the measured diffusion coefficient from that expected using Enskog kinetic theory [16,17]. The diffusion coefficient at intermediate packing fractions is enhanced compared to the theoretical value due to slowly decaying collective motions in the fluid. At densities close to crystallization, the diffusion coefficient falls below the expected value. This is attributed to cage effects as the grains are back-scattered following a collision with near neighbors [18]. Campbell [19] calculated the diffusion coefficient in a sheared cell using MD simulation techniques. He discovered that a rapidly flowing granular material is diffusive except in the limit of high packing fraction, whereupon the grains become localized and are caged by their nearest neighbors. This high density result was emphasised by the velocity autocorrelation functions not decaying monotoni-

*Electronic address: r.d.wildman@lboro.ac.uk

cally, but fluctuating with constant period as they decayed asymptotically to zero. In shear flow the diffusion coefficient manifested itself as a second order symmetric tensor, as the diffusion behavior was no longer isotropic.

In this paper, we report on an experimental study into the diffusive behavior of a two-dimensional vibrofluidized granular bed. High speed photography at framing rates of up to 3000 s^{-1}, together with automated particle tracking software, allows the mean squared displacement and granular temperature to be measured along each axis, as well as the local packing fraction. We are therefore able to make a direct assessment of the validity of the relationship between these three quantities predicted by Chapman-Enskog kinetic theory. The motivation behind these experiments is twofold: from a fundamental point of view, there is interest in the extent to which diffusive phenomena, previously observed in a thermal fluid where the collisions are elastic, are replicated in a nonequilibrium stationary state where the grains undergo inelastic collisions. Secondly, from a practical viewpoint, validating the theoretical relationship between granular temperature, diffusion constant and particle packing fraction is vital to the measurement of granular temperature in three-dimensional flows when using techniques such as positron emission particle tracking, which have insufficient time resolution to measure temperature distributions directly.

The paper is structured as follows. Section II details the experimental apparatus and arrangement. Section III describes the measurement of packing fraction and mean squared displacement obtained using high speed photography. How granular temperature and self-diffusion coefficients can be extracted from mean squared displacement curves is discussed in Sec. IV, including a brief section on measured velocity autocorrelation functions. Finally, the results and conclusions are set out in Secs. V and VI.

II. EXPERIMENTAL DETAILS

The experimental arrangement for producing and observing a two-dimensional granular gas has already been described in several previous publications [5,9,20]. In brief, a Ling dynamic systems (LDS) vibration facility consisting of an amplification system [LDS FPS 1 and PA 1000] and a broad frequency band electrodynamic transducer [LDS V651], was used to drive a glass cell containing steel spheres. When driven sinusoidally, this system has a frequency range of 5–5000 Hz, a maximum acceleration of 100 g and maximum amplitude of 12.5 mm. For the experiments described in this paper, the cell consisted of two glass parallel plates separated by 5.05 mm, confining 5 mm diameter steel ball bearings to a plane, and was vibrated at 50 Hz with an amplitude of 2.12 mm. The cell dimensions were 150 mm wide and 220 mm high. A digital camera was positioned perpendicular to the glass plates and the cell was illuminated from behind so that the grains appeared as black circles on a white background.

The motion of the steel grains was captured using a Kodak Ektapro 1000 high-speed digital camera. The camera is capable of capturing up to 1600 images at a maximum rate of 1000 frames per second when used at a full field of view of 239×192 pixels, although reduction in the number of rows of pixels allowed the camera to capture frames at rates of up to a maximum of 12 000 s^{-1}. The images were then downloaded to a Sun Ultra 170E workstation using an IEEE interface board. Image analysis software based on the Hough transform was used to measure the coordinates of each grain to a subpixel accuracy [5].

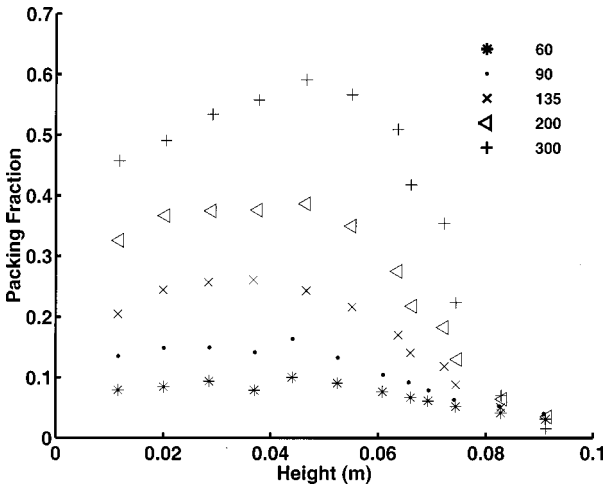

FIG. 1. Packing fraction profiles for selected numbers of grains. $N=40$, 90, 135, 200, and 300.

The number of grains in the cell, N, was varied from 40 to 500 in steps of about twenty so that a full range of packing fraction could be observed. The measured packing fraction varied from $\eta\sim0.01$ to $\eta\sim0.8$ enabling the transition from dilute to dense packing to be observed.

III. IMAGE ANALYSIS

A. Packing fraction

Packing fraction profiles are calculated from the particle coordinate data using previously established procedures [5,9,20]. The packing fraction is measured by determining the ratio of the total cross-sectional area of the spheres imaged to the total area of the field of view of the camera. Increased spatial resolution is obtained by splitting the field of view into six sections and the accuracy is improved by averaging across the width of the image. Of course, averaging over the 1600 frames of each individual experiment improves the signal to noise ratio still further. Figure 1 shows profiles of the average packing fraction as a function of the height (y) above the base of the cell for a range of values of N. The form of these curves is typical for dense vibrofluidized beds: low density near the base, rising quickly to a plateau, with an exponentially decaying tail at large y. Most of the measurements on diffusion behavior were taken over the plateau region (for example, heights 0.02 to 0.05 m for $N=200$) to avoid artefacts due to strong gradients in the packing fraction.

The influence of packing fraction is shown qualitatively in Fig. 2. Figure 2 shows typical trajectory plots at high and low packing fractions [(a) and (b), respectively]. In Fig. 2(b) the motion is chaotic whereas in Fig. 2(a) the grains tend to remain confined to ''cages'' imposed by their nearest neighbors. Block motion previously associated with the onset of convection rolls in vertically vibrated granular beds [21], is also clearly present in the top left hand corner of Fig. 2(a).

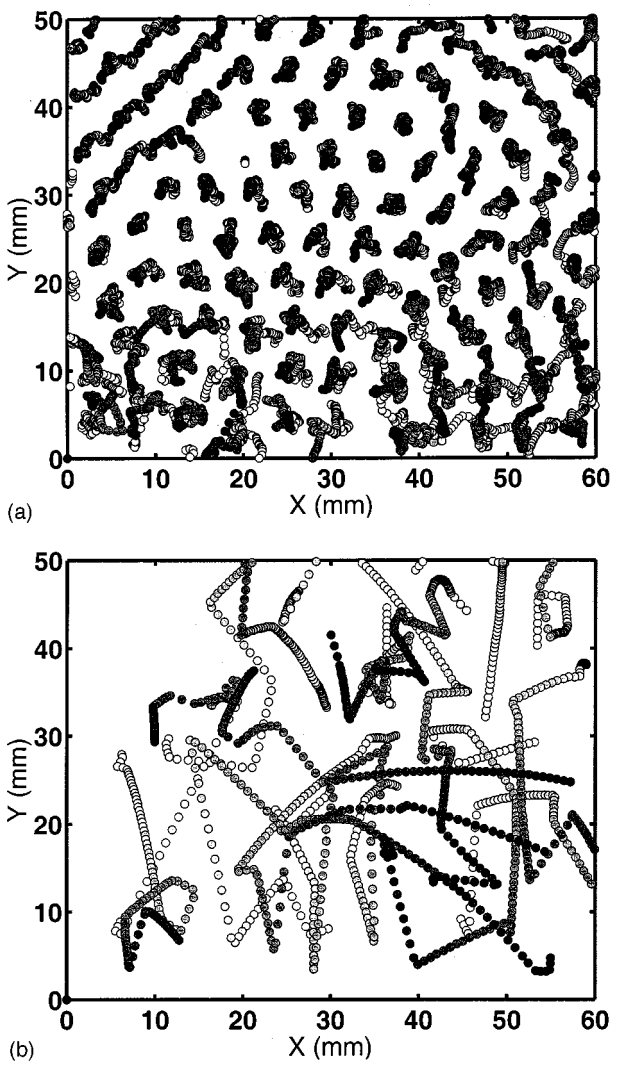

FIG. 2. Position of the grains during filming, $N=380$ (a) and $N=90$ (b). The lightening of the circles represents increasing time. Filming occurred at 1000 frames per sec; location at 1 ms intervals.

B. Mean squared displacement

The determination of the mean squared displacement starts with the location of a number of grains at $t=0$, or equivalently, in frame 1. The selected grains are tracked until one grain leaves the field of view. The mean squared displacement is then calculated at intervals of 1 ms, the framing interval of the camera. In general, a grain is lost at times significantly less than the total filming period, equal to 1.6 sec at 1000 frames per sec. A new set of grains is then selected and tracked.

To increase the effective number of grains being tracked, the 1600 images downloaded from the camera are separated into sets 200 images long, starting at consecutive frame numbers, e.g., set 1 would commence at frame 1, finishing at frame 200, set 2 would commence at frame 2 and finish at frame 201, and so on. This results in 1400 sets of images, 200 images in length. Each image is split into six horizontal segments, allowing the mean squared displacement to be measured at different heights, although the upper most and lowest segments are disregarded as the grains have a tendency to escape from the field of view at extremely short times.

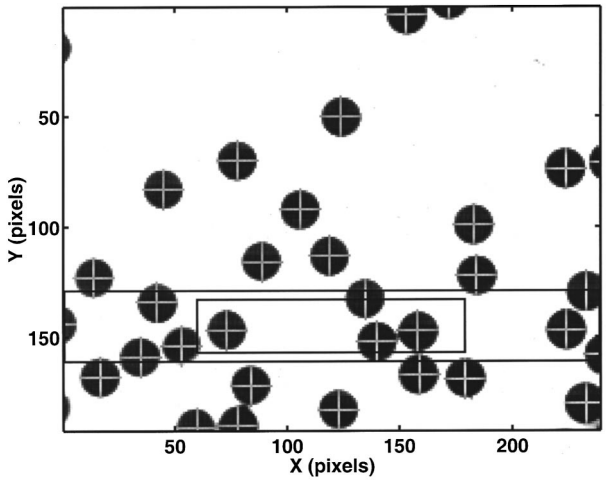

FIG. 3. High speed video crosses image of fluidized grains with detected particle position indicated by crosses. The small and large boxes represent the segment sizes used for the mean squared displacement and the velocity methods of calculating granular temperature. $N=135$, $y=55.2$ mm.

Grains are selected for tracking at the start of each set by creating a box 100 by 10 pixels (approximately $26.4\times2.7\,\mathrm{mm}^2$) at the center of each horizontal segment. Any grain located within this box at the start of each set of images is tracked until one of the grains is lost or 200 frames have been analyzed. In this way, if for example 5 grains were found within the box at each start frame, then this would result in 7000 grains being tracked in total. Figures 3 and 4 illustrate this procedure for a box at height 55.2 mm and $N=135$ grains.

Figures 5(a)–5(g) show the mean squared displacement of the grains for $N=40$, 150, 200, 300, 380, and 480 at a height of about 25 mm from the base. At low densities [Figs. 5(a)–5(c)] grains will leave the field of view before diffusive behavior is fully established (i.e., a linear relationship between mean square displacement and time is not observed).

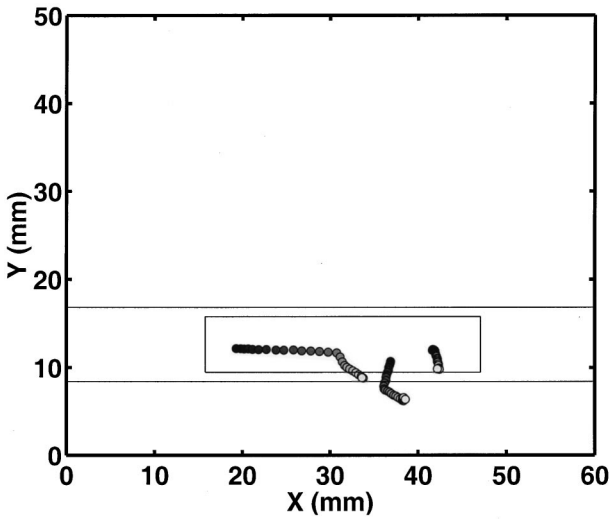

FIG. 4. Tracking of three particles located within box illustrated in Fig. 3. Particles have been tracked for 26 ms. $N=135$, $y=55.2$ mm.

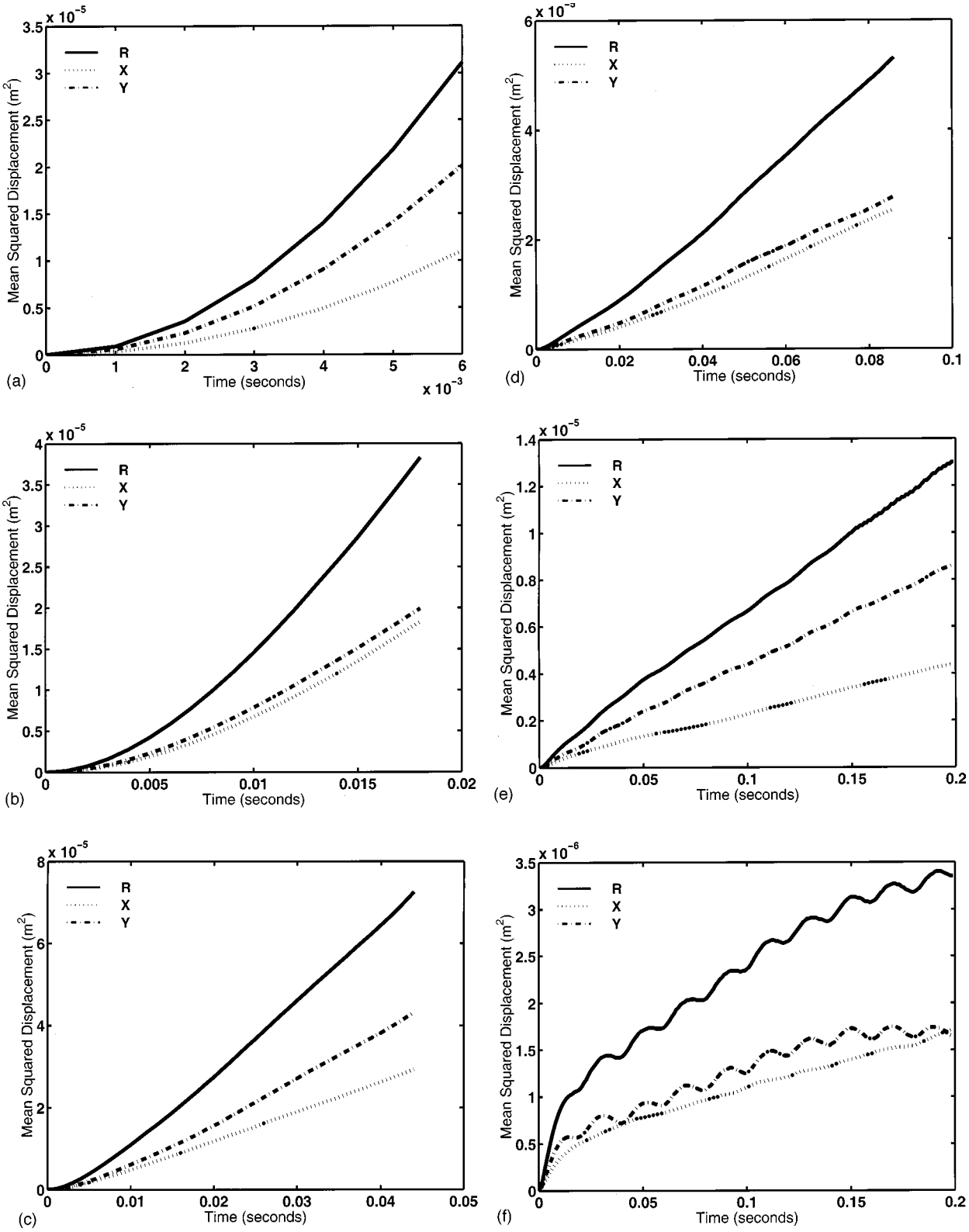

FIG. 5. Mean squared displacement behavior of $N=40$ (a), 135 (b), 200 (c), 300 (d), 380 (e), and 480 (f). Height about 25 mm from the base.

IV. CALCULATION OF *D* AND *E* FROM THE MEAN SQUARED DISPLACEMENT

Two quantities, granular temperature E and self-diffusion D were determined from the mean squared displacement. Calculation of E and D was achieved using the following three methods.

(A) At short times, $t \ll \tau_E$ (where τ_E is the Enskog mean collision time), the ballistic motion was analyzed using

$$\langle |\underline{r}(t)-\underline{r}(0)|^2 \rangle = \langle c^2 \rangle t^2, \tag{1}$$

where $\langle |\underline{r}(t)-\underline{r}(0)|^2 \rangle$ is the mean squared displacement and c is the speed of a grain. Extraction of $\langle c^2 \rangle$ from a plot of

mean squared displacement versus time using Eq. (1) leads directly to a measure of the granular temperature.

(B) At longer times, many of the grains will have suffered a collision, effectively ruling out any measure of the granular temperature. However, if $t \gg \tau_E$ then the grains may show diffusive behavior such that

$$D_m = \lim_{t\to\infty} \frac{1}{4t} \langle |\underline{r}(t) - \underline{r}(0)|^2 \rangle, \tag{2}$$

where D_m is the measured self-diffusion coefficient. In this case, the mean squared displacement is linear with time, and the self-diffusion coefficient can be determined from the gradient of a mean squared displacement versus time plot.

(C) At intermediate times, the behavior is more completely described by

$$\langle |\underline{r}(t) - \underline{r}(0)|^2 \rangle = \frac{\langle c^2 \rangle}{\beta^2} [\exp(-\beta t) + \beta t - 1], \tag{3}$$

where β is known as the friction coefficient [22].

The following sections detail, first, how method A is used to measure granular temperature over the range of packing fractions, $\eta = 0$ to 0.8, and secondly, how methods B and C are used to measure the self-diffusion coefficients over the same density range.

A. Granular temperature

In a vibrofluidized bed, the velocity distribution is typically anisotropic because energy is supplied to the grains in the vertical direction. It is therefore necessary to define a granular temperature for each direction of measurement. In this paper we define the granular temperature components E_X and E_Y, in terms of the horizontal and vertical velocity components v_X and v_Y, as

$$E_X = m\langle v_X^2 \rangle \quad \text{and} \quad E_Y = m\langle v_Y^2 \rangle, \tag{4}$$

where m is the mass of the particles and angular brackets denotes a statistical average. The velocities v_X and v_Y are measured relative to the mean velocity of the grains being tracked. The granular temperature E_o, which is determined from the distribution of speeds c, is given by

$$E_o = \frac{1}{2} m\langle c^2 \rangle = \frac{1}{2} m\langle v_X^2 \rangle + \frac{1}{2} m\langle v_Y^2 \rangle = \frac{1}{2}(E_X + E_Y). \tag{5}$$

At low packing fractions E_X and E_Y can be calculated directly from the measured velocity distribution functions. At higher packing fractions, however, this approach is less satisfactory because of the difficulty of reliably detecting all the collision events. An alternative method (method A) has been developed recently based on measurement of the mean squared displacement on time scales $t \ll \tau_E$. In the limit of $t = 0$, Eq. (1) is exact. However, small numbers of collisions will inevitably have occurred even after short times. In view of this, an estimate of $\langle c^2 \rangle$ is calculated by fitting a second order polynomial to the short time mean squared displacement behavior. The first order coefficient of this polynomial fit is then equal to the mean squared speed. This analysis is justified by consideration of the collision probabilities of the grains at short times, and is the method used in this paper to calculate the granular temperature directly [20]. This technique was validated by comparing calculation of the granular temperature by three methods, (1) fitting Maxwell-Boltzmann curves to measured velocity distributions, (2) measuring the mean squared speed directly, and (3) measurement of the granular temperature from the mean squared displacement. Even this approach cannot yield the granular temperature beyond a packing fraction of $\eta \sim 0.5$ when using the normal camera framing interval of 1 ms, since the typical mean speed of 0.5 $\mathrm{m\,s^{-1}}$ implies $\tau_E \sim 2-3$ ms. Some measurements up to $\eta \sim 0.8$ were, however, possible by reducing the interframe time to 0.333 ms, albeit at the expense of a proportionate reduction in image height.

In dilute gases the mean collision time τ_E may be calculated from the ratio of the Boltzmann mean free path λ to the mean speed $\langle c \rangle$. At high densities the shielding and volume reduction effects associated with the closely packed grains is accounted for by incorporating the radial distribution function at contact $g(d)$ such that

$$\tau_E = \frac{1}{2nd\langle c \rangle g(d)}, \tag{6}$$

where d is the diameter of the grains and n is the number density [18].

B. Self-diffusion

Equation (2) indicates that in the ideal case the self-diffusion coefficient can be measured by calculating the asymptotic gradient of the mean squared displacement with respect to time (method B). The self-diffusion coefficients in the x and y directions, D_{mX} and D_{mY}, respectively, we define as

$$D_m = D_{mX} + D_{mY} = \frac{1}{4t}(\langle |x(t) - x(0)|^2 \rangle + \langle |y(t) - y(0)|^2 \rangle), \tag{7}$$

where $\langle |x(t) - x(0)|^2 \rangle$ and $\langle |y(t) - y(0)|^2 \rangle$ are the mean squared displacements in the x and y directions after time t.

As N increases, the length of time over which the mean squared displacement can be calculated increases (Fig. 5) and diffusive behavior becomes increasingly apparent. Estimation of D_m from the gradient of this line becomes possible at $N \sim 300$. At very high values of N [Fig. 5(f)] a mode of behavior commonly called ''subdiffusive'' in the thermal fluid literature [23] becomes apparent, in which an initially steeply rising curve crosses over to a near linear behavior with a much smaller slope. Figure 5(f) shows that at $N = 480$, the motion of the grains is so strongly coupled to the motion of the shaker that even after subtracting the center of mass motion from the displacement of the grains, a sinusoidal signal is superimposed onto the mean squared displacement.

Figure 1 shows that at large heights the packing fraction becomes very small. This is accompanied by an increase in the mean free path of the grains. When the mean free path is of the order of the dimensions of the field of view of the camera, there are only a few average collision times before the tracking procedure stops. Inevitably, this means that the

system does not enter the diffusive regime, and the mean squared displacement has a broadly quadratic relationship with time. In these situations method A (ballistic analysis) is used to calculate the granular temperature, and using kinetic theory methods to be described in the following sections, we calculate the diffusion coefficient, but direct comparison of D_m with D_E (the prediction of the self-diffusion coefficient using kinetic theory, Sec. IV C) using method B is not possible. However, equating the long time result [Eq. (2)] with the long time limit of Eq. (3), allows Eq. (3) to be expressed in terms of D_m:

$$\langle |\underline{r}(t)-\underline{r}(0)|^2\rangle = \frac{D_m}{\beta}[\exp(-\beta t)+\beta t-1]. \tag{8}$$

Knowing that at long times the diffusion coefficient is related to the mean squared displacement through Eq. (8), we are able to extract D_m from the small time behavior using nonlinear regression analysis. Equation (8) is fitted to the experimental data using two parameters, D_m and β. The combination of using this method (method C) and the increase in framing rate allows the comparison of D_m to D_E to be extended to both low ($\eta<0.5$) and high ($\eta>0.7$) densities of grains.

Method C is most effective at intermediate packing fractions ($\eta=0.4-0.6$). Figure 5(d) illustrates this point. At a packing fraction of $\eta\sim 0.5$ and $N=300$ the mean squared displacement shows diffusive behavior up to a time of 0.08 seconds. This enables the fitting of Eq. (8) to both the crossover and the linear regime, which decreases the chance of fitting to a local minimum (as opposed to a global minimum) when performing the nonlinear regression. At lower packing fractions, the ballistic regime is extended, and at higher packing fractions the crossover regime diminishes to times comparable to the interframe time. Both of these events increase the likelihood of nonconvergence of the fit to the data.

The method of measuring the mean squared displacement (Sec. III B) and its analysis allows the grains to move beyond their original segment when the tracking ceases. If the tracked grains move into regions of substantially different packing fraction or granular temperature from that observed initially, then the mean squared displacement will deviate strongly from the expected asymptotic behavior predicted by Eq. (2). This has implications for the measurement of the self-diffusion coefficient. If the behavior predicted by Eq. (2) is not observed, a measurement of D_m is not taken. This approach results in a method that is ''self-correcting,'' and allows measurements to be taken only when any effect of delocalization of the grains is small.

C. Scaling of D with E

1. Self-diffusion in an isotropic medium

Using elementary kinetic theory methods [18,24], it can be shown that for a two-dimensional fluid in thermal equilibrium

$$D_E = \frac{d}{8\eta g(d)}\left(\frac{\pi E_o}{m}\right)^{1/2}. \tag{9}$$

The radial distribution function at contact can be estimated by [25]

$$g(d) = \frac{16-7\eta}{16(1-\eta)^2}. \tag{10}$$

2. Self-diffusion in an anisotropic medium

It has been established that the granular temperature in a vibrofluidized bed is anisotropic [9]. Equipartition of energy no longer holds, and in general, $E_Y > E_X$. Therefore the mean square velocity in the y direction will exceed that in the x direction, and one may expect the vertical and horizontal diffusion coefficients to differ. A rough estimate of the difference may be gained by starting from the exact relation [18]:

$$\langle |x(t)-x(0)|^2\rangle = 2\int_0^t dt' \int_0^{t'} dt''\langle v_x(t')v_x(t'')\rangle. \tag{11}$$

Within the Enskog theory of uncorrelated binary collisions [18],

$$\langle v_x(t')v_x(t'')\rangle = \langle v_x^2\rangle \exp(-|t'-t''|/\tau_E) \tag{12}$$

where it is assumed that the same Enskog mean collision time governs the decorrelation in the x and y directions. Substitution of Eq. (12) into Eq. (11) leads to

$$\langle |x(t)-x(0)|^2\rangle = 2\langle v_x^2\rangle \tau_E\{t+\tau_E[\exp(-t/\tau_E)-1]\} \tag{13}$$

which is of the same form as Eq. (3). In the long time limit, Eq. (13) leads back to Eq. (8), with

$$D_{Ex} = \frac{1}{2}\langle v_x^2\rangle \tau_E = \frac{E_x}{2m}\tau_E, \tag{14}$$

similarly

$$D_{Ey} = \frac{1}{2}\langle v_y^2\rangle \tau_E = \frac{E_y}{2m}\tau_E \tag{15}$$

and

$$D_E = D_{Ex}+D_{Ey} = \frac{1}{2m}(E_x+E_y)\tau_E$$
$$= \frac{E_o}{m}\tau_E = \frac{d}{8\eta g(d)}\left(\frac{\pi E_o}{m}\right)^{1/2} \tag{16}$$

so that Eqs. (14) and (15) may be rewritten as

$$D_{Ex} = D_E\frac{E_x}{E_x+E_y};\quad D_{Ey} = D_E\frac{E_y}{E_x+E_y}. \tag{17}$$

The Enskog theory leading to Eq. (17) does not account for correlations between successive collisions and effects of collective motion. These are included in MD simulations, which provide estimates of the ratio of D_m to its Enskog prediction D_E as a function of the packing fraction for the case of smooth, hard elastic discs [16,17].

TABLE I. Methods used to measure granular temperature and self-diffusion.

Method	Granular temperature	Self-diffusion coefficient
Method A	Directly measured using ballistic method [Eq. (1)].	Calculated using Enskog theory [Eq. (9)] following direct measurement of granular temperature.
Method B	Calculated using Enskog theory [Eq. (9)] following measurement of D_m using Eq. (2).	Directly measured using Eq. (2).
Method C	Calculated using Enskog theory [Eq. (9)] following measurement of D_m using Eq. (8).	Directly measured using Eq. (8).

A dimensionless diffusion coefficient D_o is easily generated by normalizing the diffusion coefficient by the ratio of the grain diameter squared to the mean collision time:

$$D_o = \frac{D\tau_E}{d^2} = \frac{\pi\sqrt{2}}{64\eta^2 g(d)^2}. \tag{18}$$

The dimensionless diffusion coefficients in the x and y directions, D_{ox} and D_{oy}, respectively, are calculated in the same manner and are also functions of packing fraction only. D_o was calculated using D_m and D_E substituted for D in Eq. (18) when analysing measured and predicted diffusion coefficients respectively. The methods used to measure granular temperature and self-diffusion coefficients, and the notation employed, are shown in Table I.

D. Velocity autocorrelation function

The velocity of the grains was estimated by a finite difference calculation in which the distance moved by a grain between the frame before and the frame after the current frame was divided by twice the framing interval. The cross-correlation function and the auto-correlation function for the x and y velocity components were calculated for a range of grain numbers. An example of the velocity autocorrelation function for $N=300$ and $y=20$ mm is shown in Fig. 6(a), with the short time behavior of the velocity autocorrelation function shown in Fig. 6(b). This indicates that the relaxation times in the x and y directions are similar, justifying assumptions made in Eqs. (14) and (15). At times of the order of several mean collision times the motion imparted by the shaker dominates the y-velocity autocorrelation functions as evidenced by the sinusoidal variation at a period of 0.02 sec. The x-velocity component is decoupled from the shaker motion and no such sinusoidal signal is seen superimposed on the x-velocity component autocorrelation function. In vibrofluidized beds, the velocity autocorrelation function appears to decay monotonically (for times less then the period of vibration of the base), in contrast to the predictions of Campbell [19] (albeit made for a sheared system rather than a vibrated granular medium).

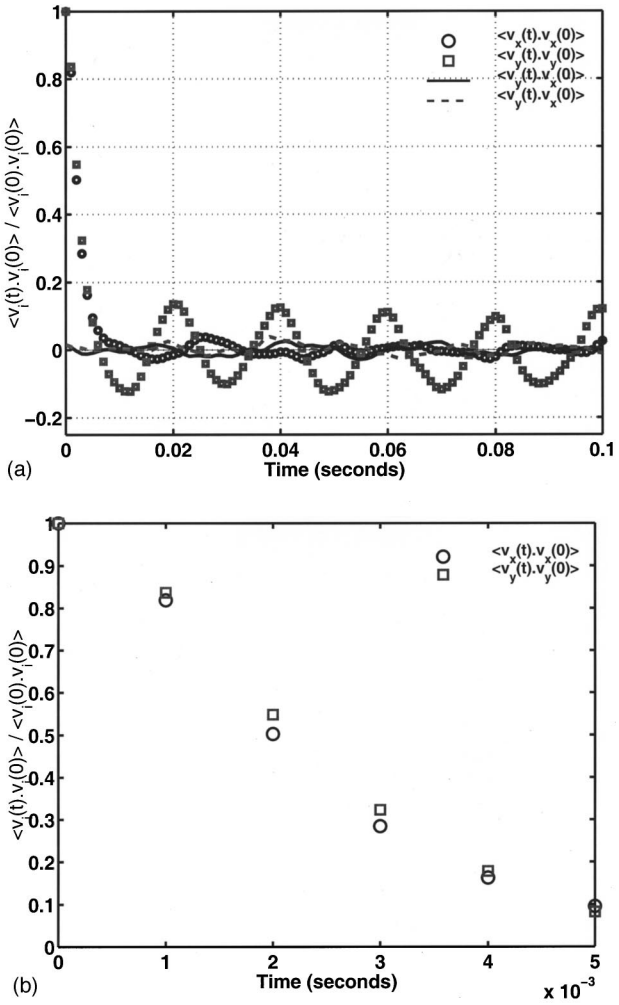

FIG. 6. Velocity correlation function. $N=300$, $y=20$ mm; (a) up to $t=0.1$ sec and (b) up to 0.06 sec.

V. RESULTS AND DISCUSSION

Figures 7(a)–7(c) show all the experimentally determined diffusion coefficients (D_m) together with the diffusion coefficients calculated, via Chapman-Enskog theory, from the measured granular temperature (D_E). The dilute phase of a granular gas is expected to behave as a nearly ideal gas at large distances from the base. In this phase the diffusion coefficient is high, reflecting the low packing fraction [Figs. 7(a)–7(c)]. In the dense phase, the diffusion is several orders of magnitude lower and approaches zero as the packing fraction approaches the 2D hexagonal close packed value ($\eta \sim 0.91$). Cage effects are also important at high densities, reducing the diffusion coefficient due to a combination of correlated collisions and enclosure. Direct measurement of the diffusion coefficient using method B was only possible above packing fractions of about 0.5 (corresponding to $N \sim 300$).

Results for both D_m and D_E fall onto a single line over the whole range of packing fractions when plotted in nondimensional form [i.e., using Eq. (18)] so as to take account of the varying mean free time between the different experiments [Figs. 7(d)–7(f)]. It should be noted that using D_E to determine D_o forces D_o to fall on to the theoretical line by definition, and also that the theoretical line for the x and y

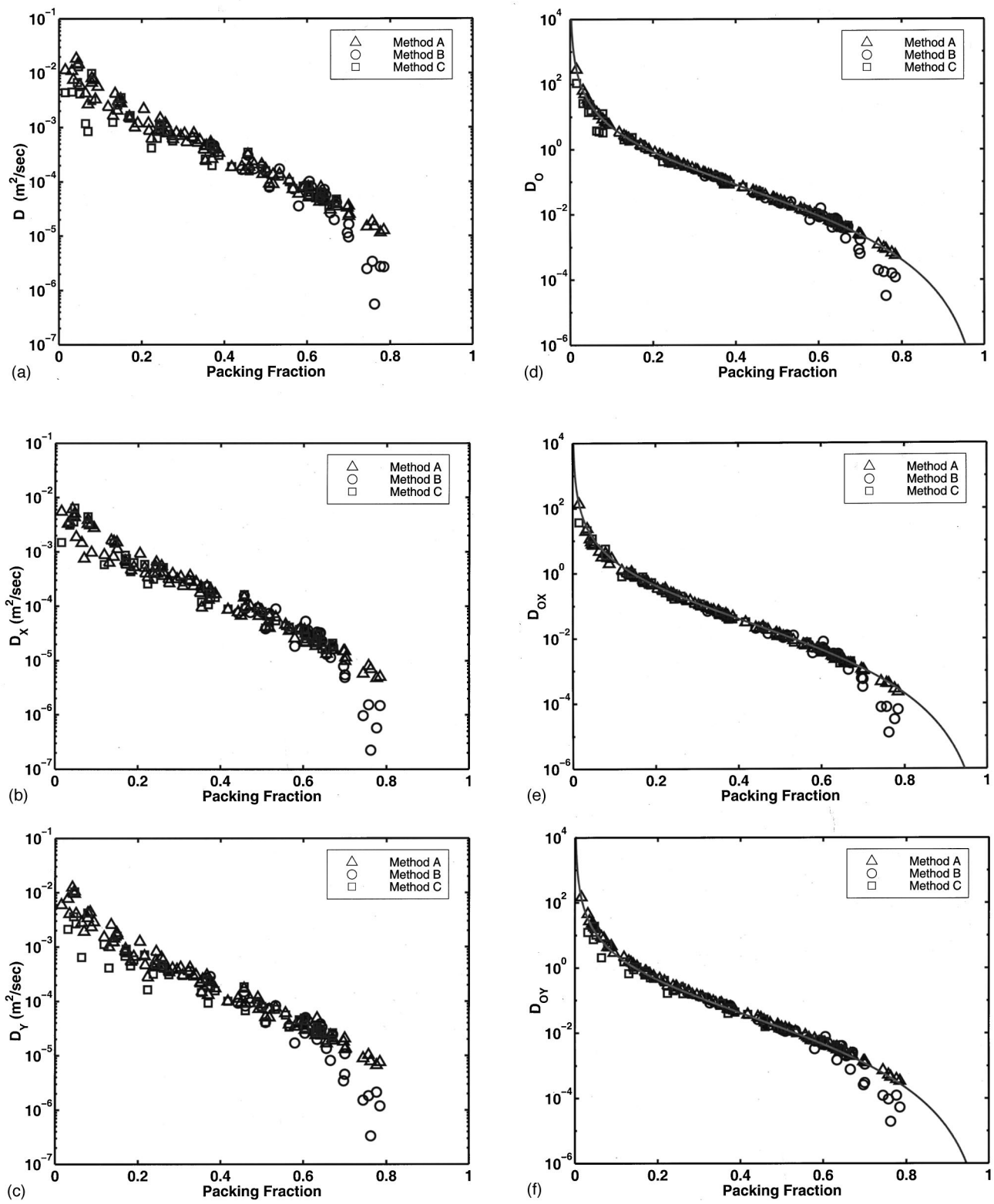

FIG. 7. Diffusion coefficient versus packing fraction: Total diffusion (a), diffusion in the x direction (b), and diffusion in the y direction (c). Dimensionless diffusion coefficient versus packing fraction: Total diffusion (d), diffusion in the x direction (e), and diffusion in the y direction (f). A: D_E. B: D_m [Eq. (2)] using Einstein relation. C: D_m [Eq. (3)].

components of diffusion are for the isotropic case. At high packing fractions D_o, D_{ox}, and D_{oy} deviate strongly from the theoretical predictions [Eq. (18)] as the collective behavior becomes more apparent, and the grains become caged. The maximum packing fraction for discs is 0.91. The diffusion coefficient is seen to drop off rapidly beyond a packing fraction of about 0.75 which is similar to observations reported in studies of discs in motion on an air table [26].

Figures 8(a)–8(f) show the granular temperature (E_X, E_Y, and E_o) vs height profiles for $N=300$ and 350 grains.

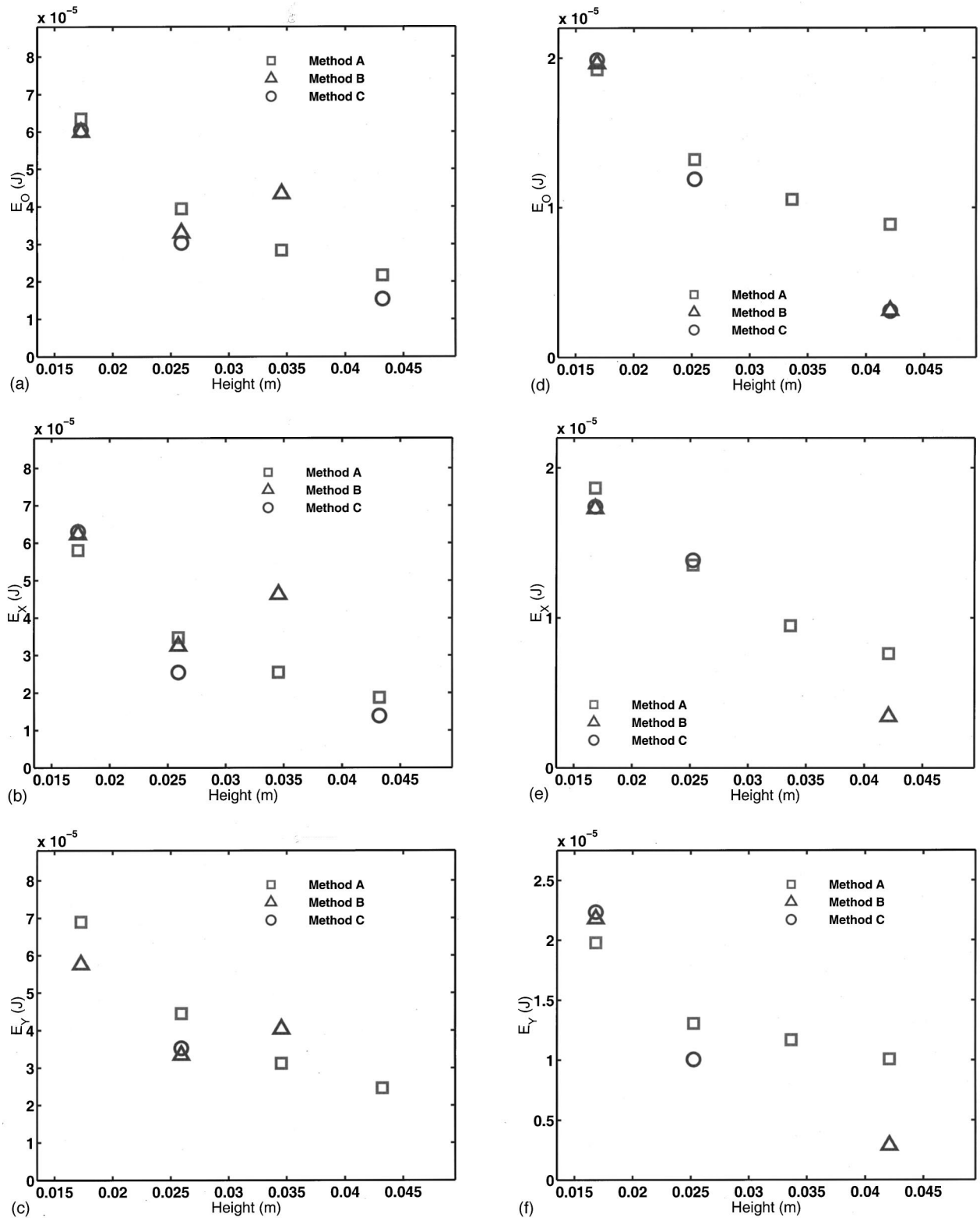

FIG. 8. Changes in the granular temperature in each direction with height; comparison of the three methods. $N=300$ (a)–(c) and 350 (d)–(f).

Good agreement between the three methods of measuring the granular temperature is observed (Table I) for these intermediate packing fractions ($\eta \sim 0.5$). The possibility arises of using molecular dynamics results from a hard disc gas to produce still closer agreement between the granular temperature measured directly (method A), and indirectly from D_m using Chapman-Enskog theory. Interestingly, such correction factors tended to shift the calculated granular temperature further from the measured values. The MD results are used under the assumption that the system is analogous to a gas of smooth, hard elastic discs. There are, of course, a number of important differences between such a model and the system

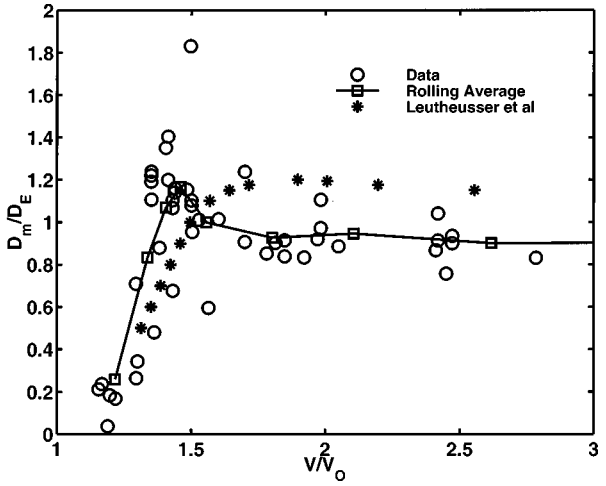

FIG. 9. Ratio of measured diffusion coefficient, D_m, to predicted diffusion coefficient, D_E. $V_0 = Nd^2\sqrt{3}/2$.

being studied here. The granular gas is not in equilibrium, there is a ''heat'' flux in the upward direction, the source being the vibrating base. One consequence of this is that the radial distribution function cannot automatically be assumed to be independent of direction, leading to anisotropy in the transport coefficients and granular temperature, and asymmetry in the velocity distributions. Consequently the system may be in a state far from that modelled in MD studies [17].

The vibrofluidized granular bed analogue to the MD results of Leuthesser *et al.* [17] is shown in Fig. 9. This shows D_m normalized by D_E, the value predicted by the Chapman-Enskog kinetic theory. The ratio is plotted as a function of the bulk volume occupied by the grains normalized by the minimum volume attainable, that is, a value of $V/V_o = 1$ indicates that the maximum packing fraction ($\eta = 0.91$) has been reached. Increases in V/V_o indicate an expansion of the bed. A rolling average of the data points shows qualitative agreement with MD results [17]. The figure suggests that above a value of $V/V_o \sim 1.3$ ($\eta < 0.7$), the measured and predicted self-diffusion coefficients are within 10–20 % of each other. At higher densities the figure suggests that diffusion drops to zero quicker than is expected from MD studies [17], and diffusion will cease to occur at a packing fraction of about 0.83.

VI. CONCLUSIONS

The present investigations show that gas kinetic theory provides broad agreement with observations on the transport and granular temperature properties of a granular bed. There are some deviations from published MD results, indicating that the assumption of near equilibrium is not always applicable in a system that is evidently in a nonequilibrium steady state. The extrapolation of the diffusion to zero seems to indicate that the cage effects may be stronger in a vibrofluidized bed than in a thermal gas. The agreement between D_m, the measured self-diffusion coefficient, and D_E, that predicted by Chapman-Enskog theory, at intermediate densities ($\eta \sim 0.5$) indicates that this method could be used at intermediate packing fractions to reliably calculate the granular temperature in situations where the velocities between collisions cannot be accurately measured.

ACKNOWLEDGMENTS

The work was funded by the Engineering and Physical Sciences Research Council under Contract No. GR/L61781, and by Shell International Oil Products B.V.

[1] H. M. Jaeger, S. R. Nagel, and R. P. Behringer, Phys. Today **49**, 32 (1996).
[2] J. T. Jenkins and S. B. Savage, J. Fluid Mech. **130**, 187 (1983).
[3] S. B. Savage, J. Fluid Mech. **92**, 53 (1979).
[4] C. S. Campbell, Annu. Rev. Fluid Mech. **22**, 57 (1990).
[5] S. Warr, G. T. H. Jacques, and J. M. Huntley, Powder Technol. **81**, 41 (1994).
[6] N. Menon and D. J. Durian, Science **275**, 1920 (1997).
[7] K. Helal, T. Biben, J. P. Hansen, Physica A **240**, 361 (1997).
[8] S. Warr and J.-P. Hansen, Europhys. Lett. **36**, 589 (1996).
[9] S. Warr, J. M. Huntley, and G. T. H. Jacques, Phys. Rev. E **52B**, 5583 (1995).
[10] V. Kumaran, Phys. Rev. E **57**, 5660 (1998).
[11] S. Luding, H. J. Herrmann, and S. Blumen, Phys. Rev. E **50**, 3100 (1994).
[12] S. McNamara and S. Luding, Phys. Rev. E **58**, 813 (1998).
[13] J. M. Huntley, Phys. Rev. E **58**, 5168 (1998).
[14] B. J. Alder and T. E. Wainwright, Phys. Rev. A **1**, 18 (1970).
[15] J. R. Dorfman and E. D. G. Cohen, Phys. Rev. Lett. **25**, 1257 (1970); Phys. Rev. A **6**, 726 (1972); **12**, 292 (1975); M. H. Ernst, E. H. Hauge, and J. M. J. van Leeuwen, Phys. Rev. Lett. **25**, 1254 (1970); Phys. Rev. A **4**, 2055 (1971).
[16] J. J. Erpenbeck and W. W. Wood, Phys. Rev. A **26**, 1648 (1982).
[17] E. Leutheusser, D. P. Chou, and S. Yip, J. Stat. Phys. **32**, 523 (1983).
[18] J. P. Hansen and I. R. McDonald, *Theory of Simple Liquids*, 2nd ed. (Academic Press, London, 1986).
[19] C. S. Campbell, J. Fluid Mech. **348**, 85 (1997).
[20] R. D. Wildman and J. M. Huntley, Powder Technol. (to be published).
[21] W. Cooke, S. Warr, J. M. Huntley, and R. C. Ball, Phys. Rev. E **53**, 2812 (1996).
[22] J. L. Doob, in *Noise and Stochastic Processes*, edited by N. Wax (Dover, New York, 1954).
[23] B. Bernu, J.-P. Hansen, Y. Hiwatari, and G. Pastore, Phys. Rev. A **36**, 4891 (1987).
[24] E. A. Guggenheim, *Elements of the Kinetic Theory of Gases* (Pergamon, Oxford, 1960).
[25] D. Henderson, Mol. Phys. **30**, 971 (1975).
[26] L. Oger, C. Annic, D. Bideau, R. Dai, and S. B. Savage, J. Stat. Phys. **82**, 1047 (1996).